NSCM005 CW 2

Part 1

Plateau bursting is a phenomenon that occurs within cells where electrical spiking activity happens due to changes in cytosolic calcium ion concentration. The bursting occurs with two phases that repeat periodically: an active phase, due to the increase in calcium concentration, and a silent phase corresponding to a decrease in calcium concentration. Bursting mechanisms occur in many different cells such as some types of neurons, where the bursting alters the release of neurotransmitters, and in pancreatic endocrine cells, where it is associated with the release of hormones such as insulin and glucagon.

In endocrine cells, plateau bursting is an essential mechanism by which the intracellular calcium concentration can be increased enough to achieve secretion of hormones [2]. The level of hormone secretion is determined by the Ca^{2+} flux into and out of the cell [4]. The mechanism relies on the interplay between voltage-gated Ca^{2+} channels and various different K^+ channel across the cell. When stimulation to the cell occurs, the membrane potential increases (becomes more positive) which in turn opens the voltage-gated Ca^{2+} channels. This causes an influx of calcium ions into the cell which activates calcium-sensitive potassium channels, which then causes potassium ions to flow out of the cell and reduces the membrane potential again. Due to the reduction of the membrane potential, the calcium channels close and the intracellular calcium concentration decreases. This then repeats and creates oscillatory behaviour in the cell membrane potential [1].

Many models of bursting behaviour have been proposed in pancreatic cells [9,10] as well as others such as neurons [8]. These models mostly create the bursting behaviour by use of the closely related dynamics of calcium of potassium channels.

The Chay-Keizer model describes plateau bursting in pancreatic islets. It was presented by T. Chay and J. Keizer in 1983 [7] as a model of pancreatic beta-cell oscillations. Given here is a reduced version of the model with fewer variables given by [5,6]. It consists of three differential equations in: *V*, the membrane potential, *n*, the fraction of activated delayed rectifier K^+ channels, and *c*, the cytosolic free Ca^{2+} concentration. These equations are shown below:

$$C_m \frac{dV}{dt} = -\left(I_{Ca} + I_K + I_{K(Ca)} + I_{K(ATP)}\right) \tag{1}$$

$$\frac{dn}{dt} = \frac{n_\infty(V) - n}{\tau_n} \tag{2}$$

$$\frac{dc}{dt} = -f(\alpha I_{Ca} + k_{PMCA} c) \tag{3}$$

Equation (1) describes the evolution of the membrane potential over time and is determined by C_m, the membrane capacitance of the cell, and four different currents of calcium and potassium ions through different channels. Equation (2) describes the change in the fraction of activated delayed rectifier K^+ channels, and is determined by the steady state activation function n_∞ (n_inf) as well as the activation time constant for this channel τ_n. Finally, equation (3) describes the evolution of the

cytosolic free Ca^{2+} concentration, involving *f*, the ratio of free to total Ca^{2+} within the cell, α, a constant to convert current to concentration flux, and k_{PMCA} which is the rate of Ca^{2+} extrusion from the cell.

There are two subsystems to note here: the fast subsystem of the variables *V* and *n*, and the slow variable *c*. We can calculate the time scale of V as: $\tau_V = {C_m}/{g_{Total}}$ where g_total is the total conductance of all the potassium and calcium channels. The values are given in [3] as $6\text{ms} \leq \tau_V \leq 24\text{ms}$, and the time scale of *n* is given as $\tau_n = 20\text{ms}$. In contrast, the slow variable *c* has a time constant $\tau_c = \frac{1}{fk_{PMCA}}$ which is equal to 8000ms with the default parameters, far larger than the *V* and *n* time scales. Therefore, there are two subsystems in play.

Part 2

The Chay-Keizer model was implemented in MATLAB. Using the default parameters given in [3], and replacing v_n=-16 with v_n=-12mV, no periodic bursting patterns were apparent at first. This is shown in Figure 1 where the model produces the first spike and some oscillatory effect that converges to one value in 1(a), and the same oscillations that continue indefinitely in 1(b).

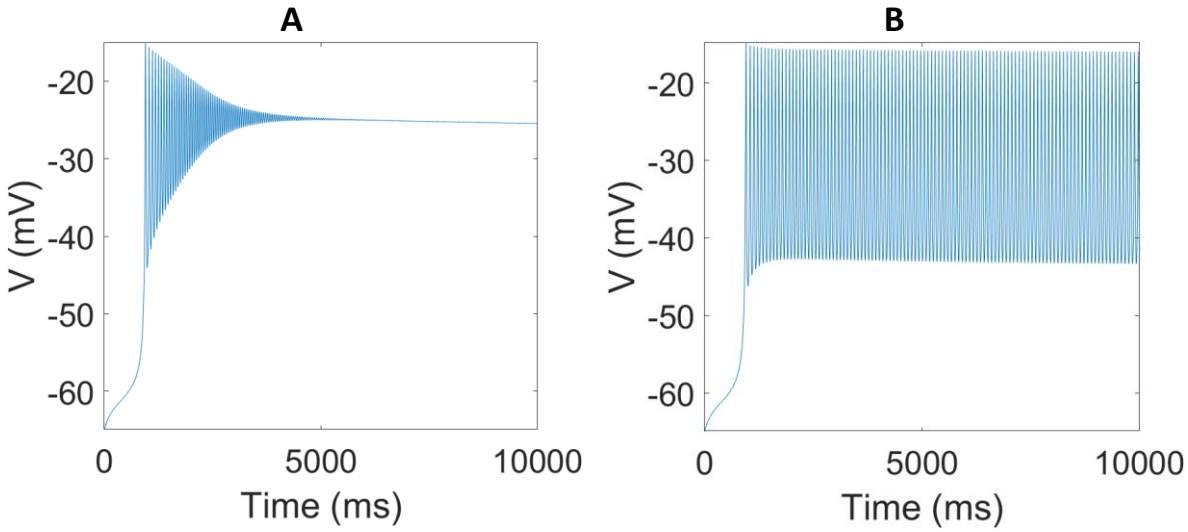

Figure 1. (**A**) The initial oscillating pattern that converges to a constant value. This is using a delta T (time) value of 0.75. (**B**) The oscillating pattern seems to continue indefinitely, with a delta T of 1.0. In both of these examples the default parameters were used (with v_n=-12mV).

This behaviour was unexpected, however indicated that parts of the system were working. Increasing the alpha parameter and tinkering with the time interval revealed the bursting behaviour as expected, shown in Figure 2.

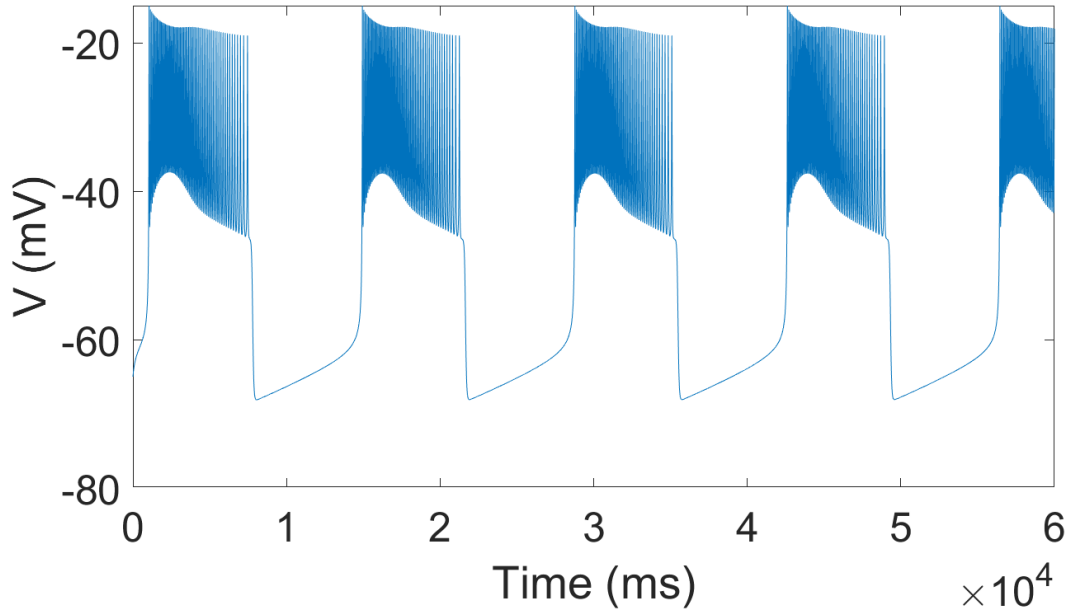

Figure 2. The periodic bursting pattern from the Chay-Keizer model using all default parameters except v_n = -12mV, and alpha = 9e-6 $fA^{-1}\mu M\ ms^{-1}$. Note the scale of the x-axis has a factor of 10^4.

Next, the model was run with varying parameters and initial conditions to investigate the effects of the different values on the bursting behaviour. Three values of the parameter *f* were used: [0.00025, 0.00050, 0.00100]. In addition, three sets of initial values were investigated too which were:

V	c	v_n
-65	0.1	-12
-50	0.7	-12
-65	0.1	-10

Figure 3 contains all the variations investigated.

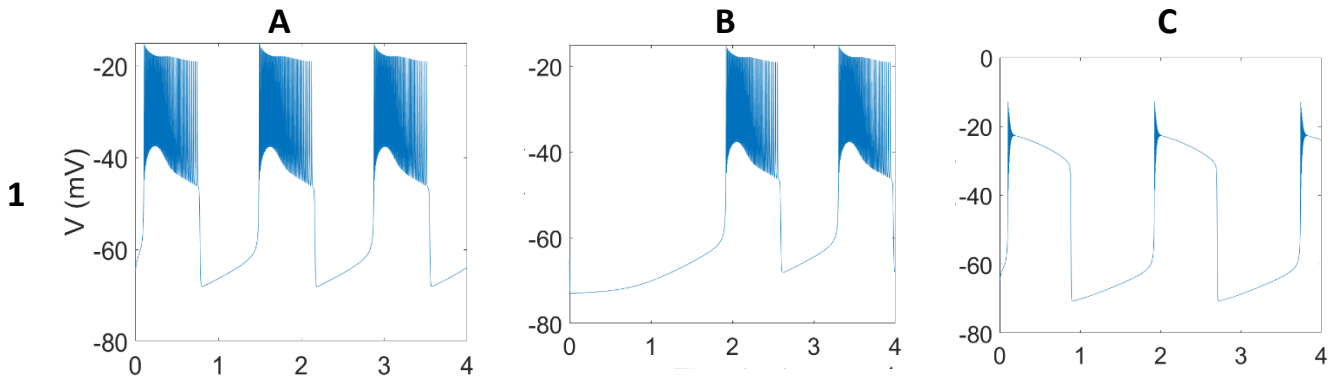

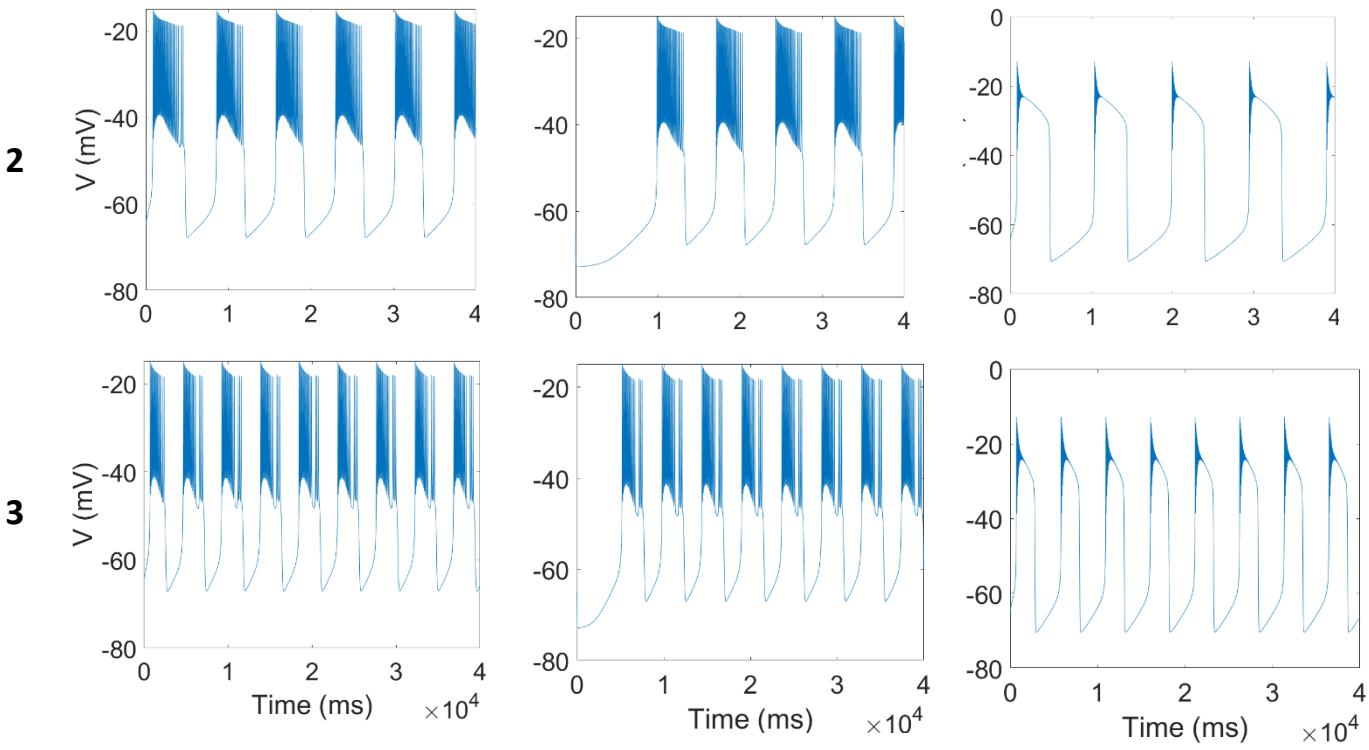

Figure 3. Displayed here are all nine combinations of the varying parameters/initial conditions. Column **A** shows plots for the initial parameters V=-65mV, c=0.1, v_n=-12mV. Column **B** uses V=-50mV, c=0.7, v_n=-12mV. Column **C** uses initial values V=-65mV, c=0.1, v_n=-10mV. Rows **1, 2** and **3** use varying values of *f* = 0.00025, 0.00050, 0.00100 respectively. All graphs use the same axes and scales.

Immediately obvious, comparing the three rows in Figure 3, is the effect of the parameter *f*. This parameter seems to increase the frequency with which the bursting patterns emerge, or, alternatively, reducing the period. This result makes sense since the *f* parameter is described as being the ratio of free to total Ca^{2+} in the cell, and so increasing this parameter will increase the amount of free Ca^{2+} and subsequently speed up the dynamics of the system. Column B shows primarily how changing the initial value of *c* impacts the system. The increase in *c* causes a delay to the beginning of the bursting oscillations. This delay is due to the time it takes for the Ca^{2+} concentration to reduce as it moves out of the cell; it hits a lower threshold as the spiking begins and the enters the oscillatory state. The values of *c* over time is shown in Figure 4.

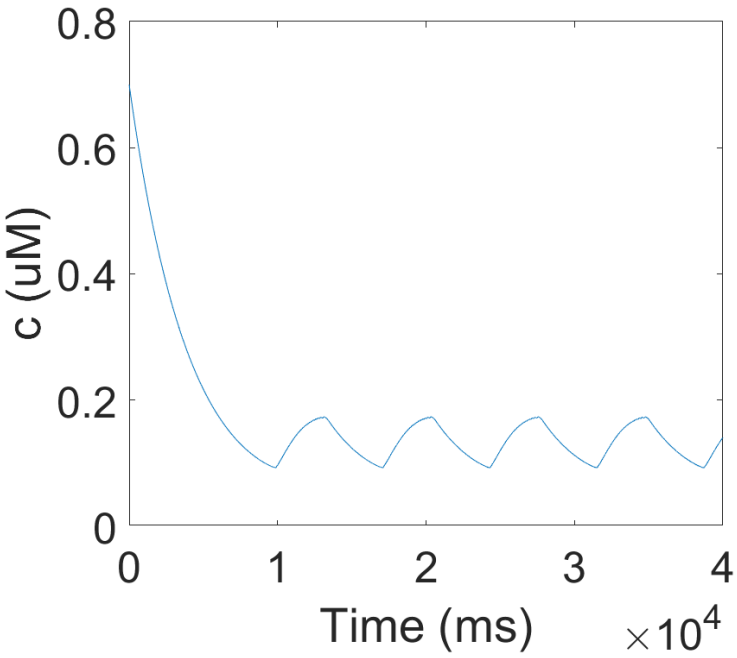

Figure 4. The slow dynamics of Ca^{2+} dynamics, illustrated with an initial value of 0.7 causing a slow decline before entering an oscillatory pattern. Other values used are initial V=-50mV, v_n=-12mV, f=0.0005. This plot is to match with Figure 3(2B).

Finally, looking down Figure 3 column C we can see the effect that v_n has on the system. Increasing v_n from -12mV to -10mV causes the oscillations to enter a more relaxed state, with reduced oscillations in each period. In [3] this is shown to be a first step in creating a pseudo-plateau bursting pattern using this model.

MATCONT was used to generate phase space diagrams to illustrate the dynamics of the system. Figure 5 and 6 show the 2D phase space of *n* and *V*, and of *c* and *V*, for an oscillation.

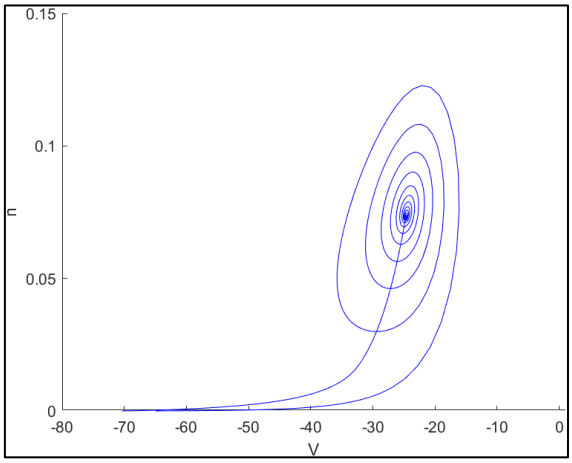

Figure 5. Phase space diagram in V and n illustrating the dynamics of the activated delayed rectifier K^+ channels in relation to the membrane potential. V is measured in mV, and n is a ratio.

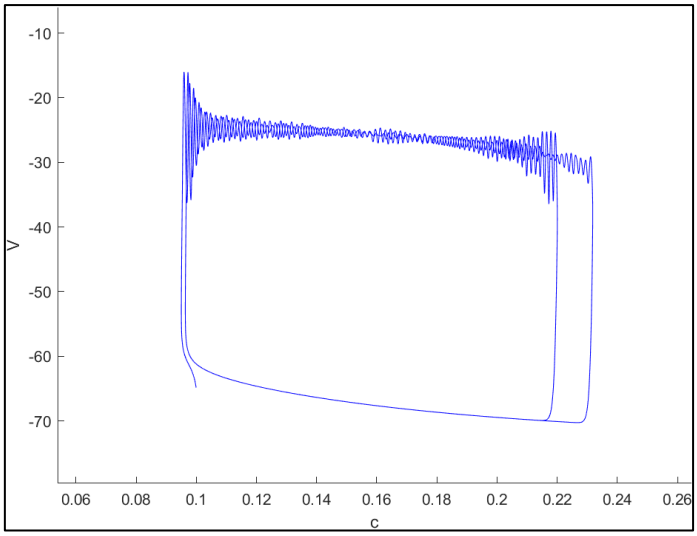

Figure 6. Phase space diagram in *c* and *V* showing the relationship between fast and slow subsystems. V is in mV and c in µM.

Most interestingly is Figure 7 which shows the full 3D phase space of all three variables interacting. The fast subsystem of *V* and *n* create spirals in the phase space as the *c* variable changes slowly back and forth. It clearly shows the two phases of activity and silence.

A

B

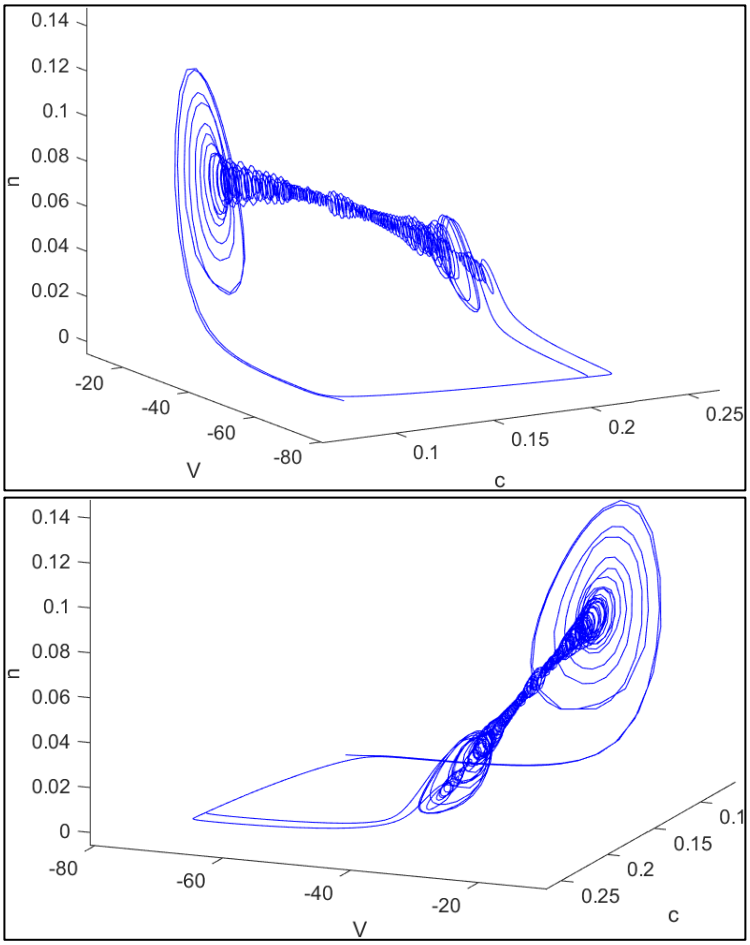

Figure 7. The 3D phase space from two different angles (A,B).

[1] Tsaneva-Atanasova, K., Osinga, H. M., Rieß, T., & Sherman, A. (2010). Full system bifurcation analysis of endocrine bursting models. *Journal of theoretical biology*, *264*(4), 1133-1146.

[2] Barg, S., & Rorsman, P. (2004). Insulin secretion: a high-affinity Ca2+ sensor after all?. *The Journal of general physiology*, *124*(6), 623-625.

[3] Teka, W., Tsaneva-Atanasova, K., Bertram, R., & Tabak, J. (2011). From plateau to pseudo-plateau bursting: Making the transition. *Bulletin of mathematical biology*, 73(6), 1292.

[4] Van Goor, F., Zivadinovic, D., Martinez-Fuentes, A. J., & Stojilkovic, S. S. (2001). Dependence of pituitary hormone secretion on the pattern of spontaneus voltage-gated calcium influx. *Journal of Biological Chemistry*, 276(36), 33840-33846.

[5] Bertram, R., & Sherman, A. (2004). A calcium-based phantom bursting model for pancreatic islets. *Bulletin of mathematical biology*, 66, 1313-1344.

[6] Bertram, R., & Sherman, A. (2005). Negative calcium feedback: the road from Chay–Keizer. *In S. Coombes, & P. Bressloff (Eds.),* The genesis of rhythm in the nervous system (pp. 19–48). New Jersey: World Scientific Press.

[7] Chay, T. R., & Keizer, J. (1983). Minimal model for membrane oscillations in the pancreatic beta-cell. Biophysical journal, 42(2), 181-189.

[8] Hindmarsh, J. L., & Rose, R. M. (1984). A model of neuronal bursting using three coupled first order differential equations. Proceedings of the Royal society of London. Series B. Biological sciences, 221(1222), 87-102.

[9] Bertram, R., Previte, J., Sherman, A., Kinard, T. A., & Satin, L. S. (2000). The phantom burster model for pancreatic β-cells. Biophysical journal, 79(6), 2880-2892.

[10] Bertram, R., & Sherman, A. (2004). A calcium-based phantom bursting model for pancreatic islets. Bulletin of mathematical biology, 66, 1313-1344.

MATLAB Code:

```
% NSCM005 CA2 - the Chay-Keizer model of plateau bursting in endocrine
% cells

% Define parameters
DT = 0.9; % time step, [ms]
T_MAX = 40000; % max time, [ms]

g_Ca = 1000; % maximum conductance of Ca channel [pS]
g_KCa = 400; % maximum conductance of K(Ca) channel [pS]
g_K = 2700; % maximum conductance of K channel [pS]
g_KATP = 180; % maximum conductance of K(ATP) channel [pS]
V_Ca = 25; % [mV]
V_K = -75; % [mV]
C_m = 5300; % [fF]
tau_n = 18.7; % [ms]
alpha = 9e-6; % [fA^-1 uM ms^-1]
f = 0.00025; % [-]    % 3 different values
k_PMCA = 0.5; % [ms^-1]
K_d = 0.3; % [uM]
v_n = -12; % [mV]
v_m = -20; % [mV]
s_n = 5; % [mV]
s_m = 12; % [mV]

% Declare/allocate variables
num_steps = round(T_MAX/DT); % number of time steps [-]

V = zeros(num_steps, 1);
n = zeros(num_steps, 1);
c = zeros(num_steps, 1);
I_K = zeros(num_steps, 1);
I_KATP = zeros(num_steps, 1);
I_Ca = zeros(num_steps, 1);
I_KCa = zeros(num_steps, 1);


% Initial conditions
V(1) = -65;
n(1) = 0.0;
c(1) = 0.1;
I_K(1) = 0;
I_KATP(1) = 0;
I_Ca(1) = 0;
I_KCa(1) = 0;
v_n = -12;

% Main Loop
for i = 2:num_steps

    % calculate activation functions
    m_inf = ( 1+exp((v_m-V(i-1))/s_m) )^-1;
    n_inf = ( 1+exp((v_n-V(i-1))/s_n) )^-1;
    s_inf = c(i-1)^3/(c(i-1)^3+K_d^3);

    % calculate currents
```

```
    I_K(i) = g_K*n(i-1)*(V(i-1)-V_K);
    I_KATP(i) = g_KATP*(V(i-1)-V_K);
    I_Ca(i) = g_Ca*m_inf*(V(i-1)-V_Ca);
    I_KCa(i) = g_KCa*s_inf*(V(i-1)-V_K);

    % calculate variable changes
    DV = -1/C_m*(I_Ca(i)+I_K(i)+I_KCa(i)+I_KATP(i))*DT;
    Dn = 1/tau_n*(n_inf-n(i-1))*DT;
    Dc = -f*(alpha*I_Ca(i)+k_PMCA*c(i-1))*DT;

    % update values
    V(i) = V(i-1)+DV;
    n(i) = n(i-1)+Dn;
    c(i) = c(i-1)+Dc;
end



% Plotting
t = 0:DT:(num_steps-1)*DT;

subplot(1,2,1);
plot(t,V);
set(gca,'FontSize',24);
xlabel('Time (ms)');
ylabel('V (mV)');
ylim([-80 0]);

subplot(1,2,2);
plot(t,c);
set(gca,'FontSize',24);
xlabel('Time (ms)');
ylabel('c (uM)');
ylim([0.06 0.2]);
```